Hindawi Publishing Corporation
International Journal of Photoenergy
Volume 2013, Article ID 178017, 9 pages
http://dx.doi.org/10.1155/2013/178017

*Research Article*

# Optical and Electrical Properties of Thin Films of CuS Nanodisks Ensembles Annealed in a Vacuum and Their Photocatalytic Activity

**J. Santos Cruz,[1] S. A. Mayén Hernández,[1] F. Paraguay Delgado,[2] O. Zelaya Angel,[3] R. Castanedo Pérez,[4] and G. Torres Delgado[4]**

[1] *Facultad de Química, Materiales Universidad Autónoma de Querétaro, 76010 Querétaro, QRO, Mexico*
[2] *Centro de Investigación en Materiales Avanzados S.C., Miguel de Cervantes 120, 31109 Chihuahua, CHIH, Mexico*
[3] *Departmento de Física, CINVESTAV, Apartado, Postal 14-740, 07000 México, DF, Mexico*
[4] *Cinvestav-IPN, Unidad Querétaro, Apartado Postal 1-798, 76230 Querétaro, QRO, Mexico*

Correspondence should be addressed to J. Santos Cruz; jsantos@uaq.edu.mx

Received 25 May 2013; Revised 9 August 2013; Accepted 12 August 2013

Academic Editor: Niyaz Mohammad Mahmoodi



Effects on the optical, electrical, and photocatalytic properties of undoped CuS thin films nanodisks vacuum annealed at different temperatures were investigated. The chemical bath prepared CuS thin films were obtained at 40°C on glass substrates. The grain size of 13.5 ± 3.5 nm was computed directly from high-resolution transmission electron microscopy (HRTEM) images. The electrical properties were measured by means of both Hall effect at room temperature and dark resistivity as a function of the absolute temperature 100–330 K. The activation energy values were calculated as 0.007, 0.013, and 0.013 eV for 100, 150, and 200°C, respectively. The energy band gap of the films varied in the range of 1.98 up to 2.34 eV. The photocatalytic activity of the CuS thin film was evaluated by employing the degradation of aqueous methylene blue solution in the presence of hydrogen peroxide. The CuS sample thin film annealed in vacuum at 150°C exhibited the highest photocatalytic activity in presence of hydrogen peroxide.

## 1. Introduction

Since the prediction by Feynman about the importance of nanotechnology as early as 1959, semiconductor chalcogenide nanocrystals became fundamentally interesting due to their captivating size properties and their subsequent applications. The effects determined by the crystal size in the evolution of thermodynamic, structural, spectroscopic, electromagnetic, electronic and chemical properties result in a class of materials with unusual properties, which are dependent on the size, generating significant changes in both surface and electronic properties of the materials. Considering the importance of nanocrystals in technological applications, a large number of requests of the chalcogenides in electro- and absorbing coatings [1–7], selective radiation filters in architectural windows [8], electrodes [9], chemical sensors [7, 10], optoelectronic devices [11], thermoelectric cooling materials [12], and catalysts [13, 14], among others, are expected. Numerous studies have been reported on the CuS binary system in powder, bulk, and as thin films with different compositions and properties. These differences in the properties originated mainly by factors related to phases equilibria, because of a strong tendency of Cu and S to form several metastable and nonstoichiometric phases. The copper chalcogenide ($Cu_xS$) system is known to have five different stable phases at room temperature: chalcocite ($Cu_2S$), djurleite ($Cu_{1.95}S$), digenite ($Cu_{1.8}S$), anilite ($Cu_{1.75}S$), and covellite (CuS) [15–18] with a crystal structure varying from hexagonal to orthogonal.

Several techniques have been utilized in order to obtain $Cu_xS$ thin films; the more common are solvothermal method [12], atomic layer deposition [19], hydrothermal [20], photo chemical deposition [21], sonochemical [22], microwave [23], solid state reaction [24, 25], metalorganic deposition [26], vacuum evaporation [19, 27], microemulsion [28], spray

pyrolysis [29–31], polyol route [32], and chemical bath deposition (CBD) [3, 4, 33, 34]. The CBD is a cheap and powerful technique for preparing thin film materials at atmospheric pressure and low temperature (less than 95°C). With this method it is possible to make large area thin films in any type of substrate and of almost any shape.

The CuS is a base material for the formation of novel quaternary compounds, hence the interest in knowing their optical, morphological, and electrical basic properties. In this work, thin films of CuS nanodisks ensembles were prepared by CBD; after growth the samples were thermally annealed in vacuum (VA) at 100, 150, and 200°C. Nanoimages of high resolution were obtained and demonstrated the nanocharacter of the samples. Electrical measurements show good electrical properties and p-type CuS semiconductors and optical characterization reveals good transmittance values. With these physical properties we have found that our material has excellent photocatalytic properties as proven in the hydrogen peroxide assisted photobleaching of methylene blue aqueous solutions.

## 2. Experimental Procedure

The CuS thin films were grown on glass slides as substrates by the CBD technique at 40°C during 60 min. The substrates were washed with soap (Extran) and a soft fiber and then rinsed with distilled and deionized water; after that the substrates were placed in a chromic acid solution for 24 h. Then, the substrates were rinsed with deionized water several times and chemically attacked in a water-nitric acid solution 1 : 3, respectively, for 3 hours at slowly boiling. The glass slides were immersed vertically in an aqueous solution containing copper sulfate ($CuSO_4{\cdot}5H_2O$, 0.01 M), sodium acetate ($CH_3COONa$, 0.002 M), triethanolamine [$(HOCH_2CH_2)_3N$, 5.2 mL], and thiourea ($(NH_2)_2CS$, 0.005 M). Highly pure water (~18 MΩ) was used for the solution. The temperature was controlled by means of a hot plate equipped with magnetic stirring at 40 ± 1°C. After the growth, the thin films were rinsed in highly pure water by ultrasonic cleaning for 10 min; immediately after the rinse, the films were thermally annealed in a vacuum chamber at a pressure of $5 \times 10^{-6}$ Torr at the following thermal annealing temperatures ($T_a$) of 100, 150, and 200°C during 50 minutes for all samples and slowly cooled in the chamber.

Transmission electron microscopy (TEM) apparatus employed was a Jeol 2010 working at 200 keV. CuS layers were detached from the substrate and attached onto the TEM-grills. Scanning transmission electron microscopy (STEM) JEM-2200FS indexation was computed by $d = \lambda L/r$ where the electron wavelength at 200 keV was $\lambda = 0.0027$ nm, a steady camera for diffraction was used, $L = 30$ cm, and $r$ (mm) was the radius measured from a transmitted electron beam to the diffracted rings, Figure 1. Data from selected area electron diffraction (SAED) and XRD were taken to define the structure by Diamond 3.0 software. The ultraviolet-visible (Uv-Vis) spectra of the films were measured on a Perkin-Elmer Lambda-2 spectrophotometer using a noncoated glass in the reference beam. Measurements of atomic concentration of elements were achieved by means of the electron dispersion spectroscopy (EDS) technique utilizing a Philips XL30-ESEM. The thickness was measured on a Sloan Dektak IIA. The electrical properties in darkness were measured as a function of temperature using a conventional two-point system, with a heating rate of 0.15 K/s from 100 to 450 K with an applied bias voltage of 10 V on equipment made in our laboratory. The conductivity and Hall characterization was measured at ambient temperature with Ecopia HMS-300 four-point method. The photocatalytic activity test was determined starting from 3.5 mL of methylene blue aqueous solution (MB), at $2 \times 10^{-5}$ mol/L concentration, 0.25 $\mu$L of hydrogen peroxide at 50% w/w and CuS nanodisks thin film were placed in a quartz cell of 1 cm × 1 cm × 4 cm dimensions and irradiated with a germicidal commercial lamp ($\lambda = 252$ nm, 11 W). In the interior of the quartz cell a rectangular sample of area, 2 $cm^2$, was inserted. The reaction vessel was fixed at 4.5 cm to the irradiation lamp. The irradiation times were 1 up to 10 minutes in steps of one minute; the residual concentration was quantified by Uv-Vis spectroscopy absorption with previous external calibration standards (2, 1.5, 1.0, 0.5, and $0.25 \times 10^{-5}$ mol/L) at 663 nm.

## 3. Results and Discussion

The as-deposited and vacuum-annealed samples were smooth, highly adherent to the substrate, and free of pinholes. Representative HRTEM images of the CuS thin films prepared at 40°C by the chemical bath deposition technique and the subsequent annealing in a vacuum atmosphere are illustrated in Figure 1. In this figure the morphology and crystalline nature of CuS nanodisks are shown by the SAED pattern (see inset of Figure 1(a)). The high resolution of the diffraction rings is clearly indicative of the nanocrystallinity of the thin films. The structure consisted of the overlapped nanoplates as signposted in Figures 1(b) and 1(c), which have the main faces parallel to the substrate. Also, observe the different orientations that the nanoplates have from one grain to another, which shows the polynanocrystalline grain character. Figure 1(d) shows nanodisks oriented side to side and with the edges perpendicular to the substrate and forming linear chains. Extended linear chains assemblies are typical for CuS nanostructures [35, 36]. The CuS nanodisks stacked on their sides with several structural defects could be due to the particular orientation (parallel sides to the substrate) and the Moire interference is clearly shown in Figures 1(d) and 1(c), these patterns revealed the crystallinity of each grain because it shows different interplanar distances. Similar modulated fringes have been observed in graphene and silicon [37, 38].

The fit to the grain size (by considering spheres as an approximation) histogram is performed with Gaussian line shapes and is shown as a solid line in Figure 2. The histogram of nanoparticle grain size distribution shows the average diameter of the grains; this value is represented by the peak position of the Gaussian curve of the histogram, that is, 13.5 ± 3.5 nm (Figure 1(b)).

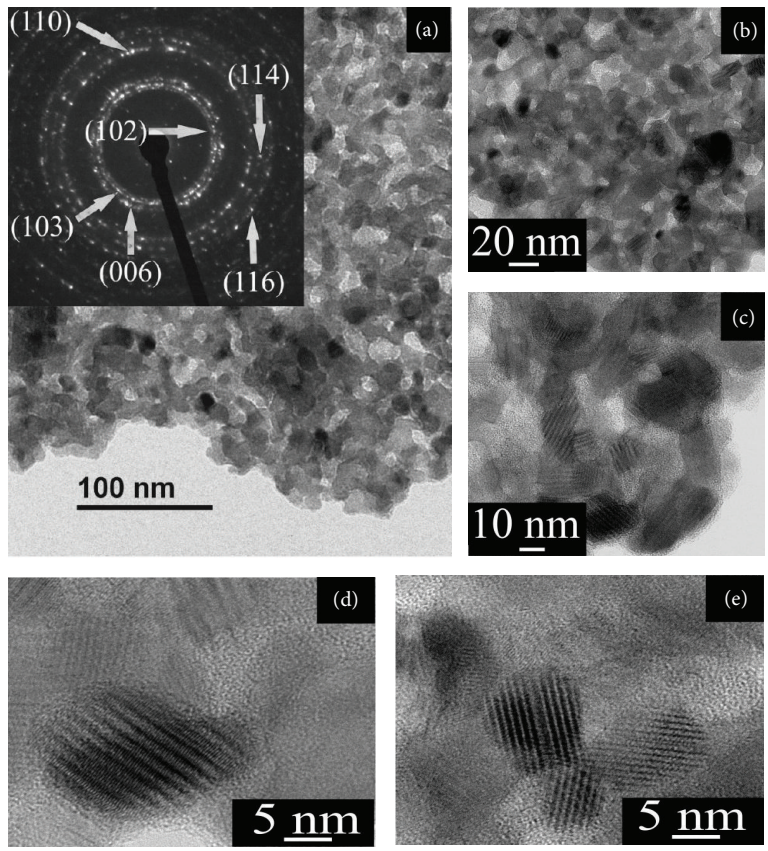


Figure 1: HRTEM images of nanodisks of CuS. (a) Low magnification HRTEM image of representative copper sulfide nanocrystals (inset: corresponding SAED pattern); (b), (c), (d), and (e) higher magnification images of the portion of the CuS with columns of nanodisks with the edges oriented perpendicular to the substrate.

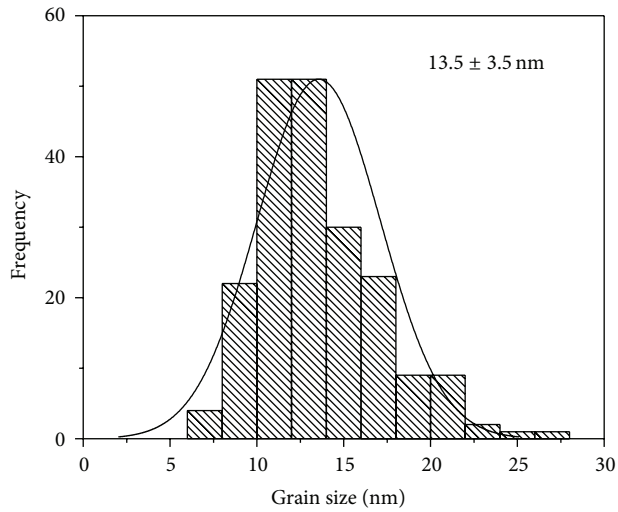


Figure 2: Histogram distribution of grain size of CuS thin film.

The X-ray patterns of the samples annealed in a vacuum atmosphere are shown in Figure 3. The data analysis shows the single covellite phase with hexagonal crystalline structure; the diffractions peaks at $2\theta$ values of 29.27°, 31.78°, and 47.92° can be indexed as (102), (103), and (110) reflections of the hexagonal phase CuS, with (110) as the preferential crystalline direction, which are well matched with the standard values (JCPDS 74-1234). The crystallinity is improved as the annealing temperature increases.

The porous nature of volume of films can be observed from the STEM image of Figure 4 (see Figure 1(a)), which indicates that nanodisks are randomly oriented in the space. The influence of the annealing vacuum atmosphere and temperature on the electrical properties of the CuS samples was estimated by the Hall effect technique with aluminum dot contacts at equidistant distances in a square sample of the 1 $cm^2$ with Van der Pauw configuration. In order to test the metallic contacts, we obtained a linear graph of current ($I$) versus voltage ($V$) (not shown), which indicates that the aluminum acts as an ohmic contact.

The distance between next contact points was 0.8 cm. Hall measurements were carried out at room temperature (298 K) with a constant current of 100 $\mu$A and with a magnetic field of 0.5 Tesla. All the samples exhibited p-type conductivity. The results are shown in Figure 5: the resistivity ($\rho$), the holes concentration ($p$), the mobility ($\mu$), the sheet concentration ($S_{[\,]}$), the Hall coefficient ($R_H$), and the thickness ($d$); $\rho$ and $\mu$ decrease, in general, as $T_a$ increases (Figure 5(a)); because of the formation of defects inside the material, majority defects

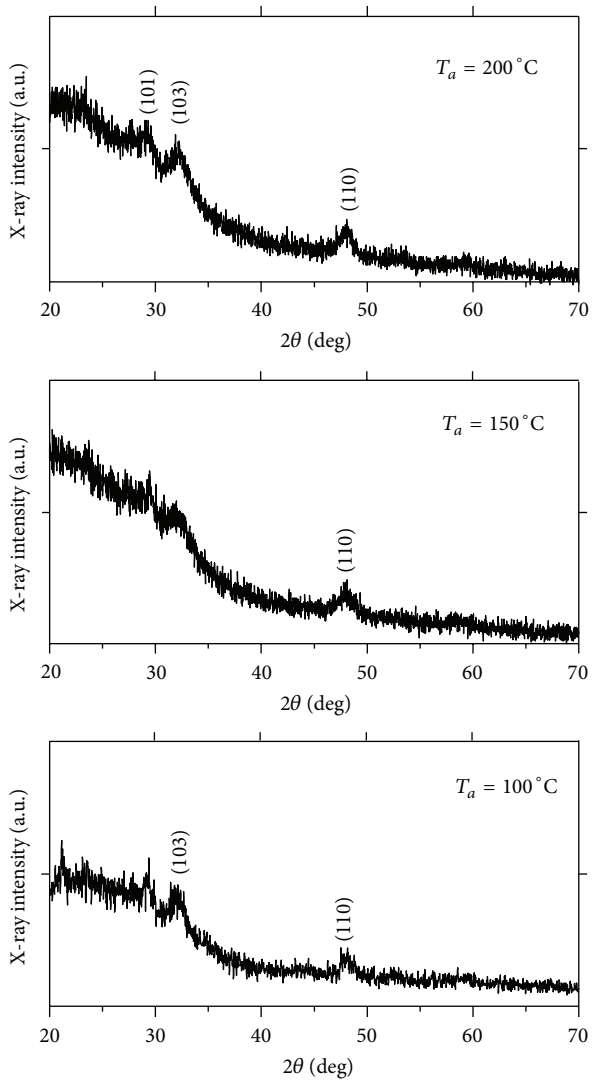


Figure 3: XRD patterns of the samples annealed in a vacuum atmosphere.

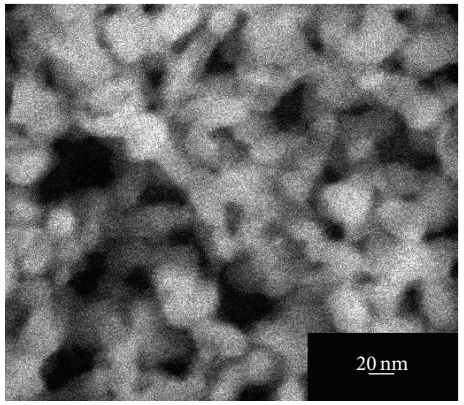


Figure 4: STEM image of a CuS thin film.

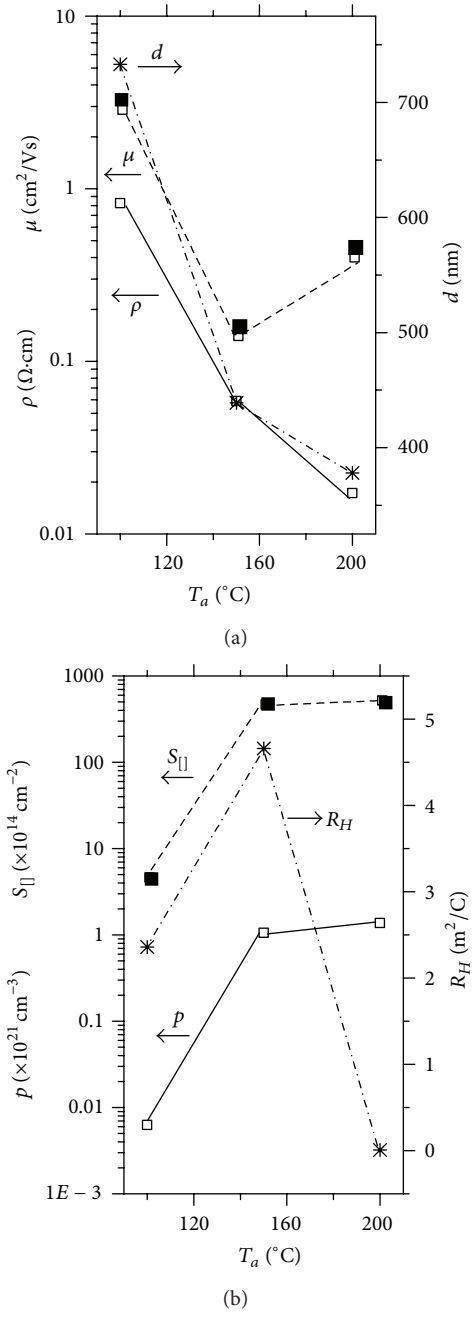


Figure 5: (a) Resistivity ($\rho$), mobility ($\mu$), and thickness ($d$) as a function of the annealing temperature ($T$). (b) Sheet concentration ($S_{[]}$), holes concentration ($p$), and Hall coefficient ($R_H$) versus $T$.

should be Cu vacancies ($V_{Cu}$). The material tends to grow with a deficiency of copper (Cu-poor). This was also observed by Adelifard et al. [7]. $V_{Cu}$'s have a negative net charge, and then trap holes that can be ionized easily with temperature, which becomes the CuS films p-type.

The decrease in resistivity after the annealing treatment in vacuum (see Figure 5(a)) is due to the increase in the majority carrier concentration. Hall mobility depends on (i) crystallinity, (ii) both grain size and their orientation,

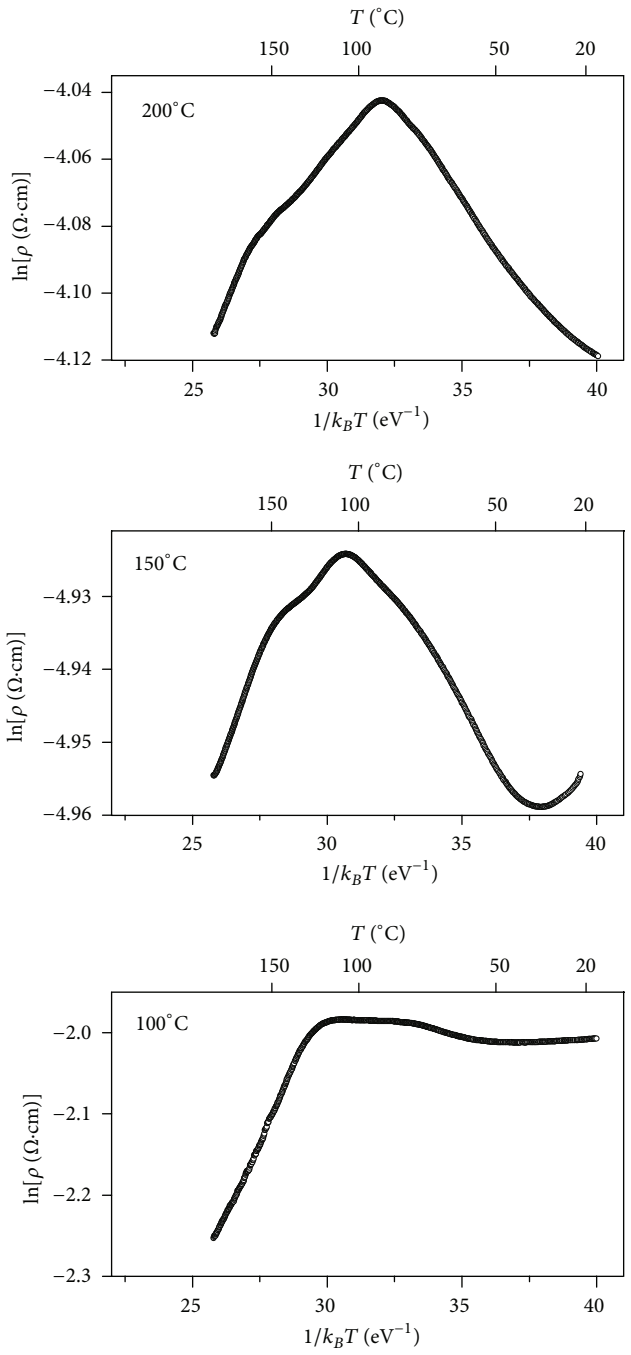


FIGURE 6: Reciprocal temperature dependence of electrical resistivity of CuS thin films annealed in vacuum at 100, 150, and 200°C.

and (iii) texture [39, 40]. In the chemical bath technique the postannealing processes are the main factors that affect the morphology, structural and electrical properties. In the present study, we have observed that the vacuum annealing improves the conductivity; however, this affects significantly the mobility due to the fact of the reduction of drift velocity and mean free path [41]. As $R_H \propto -\mu\rho$, if both $\mu$ and $\rho$ decrease, $R_H$ decreases. The electrical resistivity of CuS as a function of absolute temperature (293–350 K, 20–180°C) is

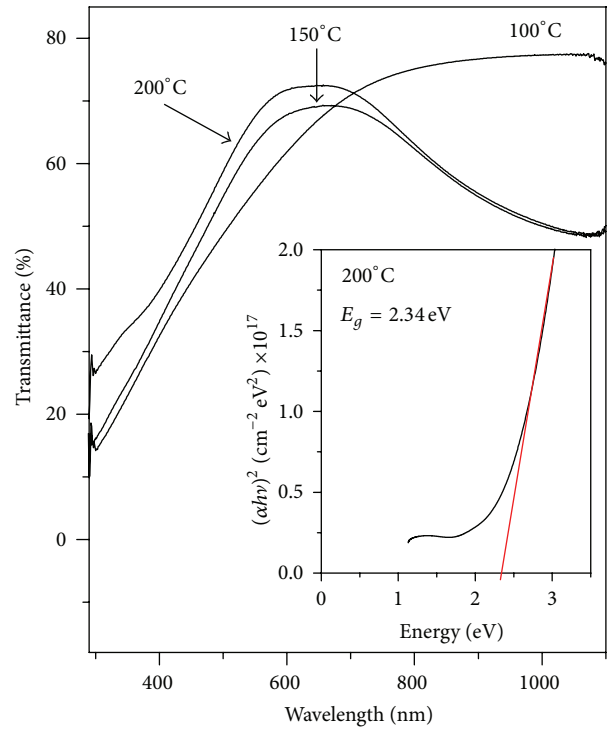


FIGURE 7: Optical transmittance spectra of CuS thin films annealed in a vacuum atmosphere. Inset plot of the $(\alpha h\nu)^2$ versus $h\nu$ for CuS thin film with $T_a = 200$°C.

shown in Figure 6 for the three samples studied. In general, the resistivity of semiconductors follows the equation

$$\rho = \rho_0 \exp\left(\frac{-\Delta E}{k_B T}\right), \quad (1)$$

where $k_B$ is the Boltzman constant, $T$ is the absolute temperature, $\rho_0$ is the resistivity when $1/k_BT = 0$, and $\Delta E$ is the activation energy. In Figure 6, it can be observed that all the films exhibited an approximated straight-line behavior in the interval $32 \leq 1/k_BT \leq 40$, in which $\rho$ decreases when $T$ increases, as expected in semiconductor material. The average activation energies calculated from the slope of the ln ($\rho$) versus $1/k_BT$ are 0.007, 0.013, and 0.013 eV for $T_a = 100$, 150, and 200°C, respectively. The activation energy 0.013 eV could be attributed to the shallow acceptor states due to Cu vacancies at 0.012 eV [42]. For $1/k_BT < 31$ ($T > 100$°C), in the three samples, CuS experiences a transformation from semiconductor to metallic-like material; the resistivity increases when $T$ increases, such as occurs for highly conductive semiconductors.

The optical transmittance of CuS thin films in the wavelength range 350–1100 nm is exhibited in Figure 7. The CuS film annealed at 100°C resulted with the highest transparency (≈70%), and the transmission decreases lightly ≈10% with the increase $T_a$ (≈60%). The optical band gap ($E_g$) was estimated using the Tauc model, extrapolation of the linear portion of the plots $(\alpha h\nu)^2$ versus $h\nu$ to $\alpha = 0$, that is, the energy axis. For $T_a = 200$°C, $E_g$ calculation can be observed in the inset of Figure 7. The direct band gap values of the samples

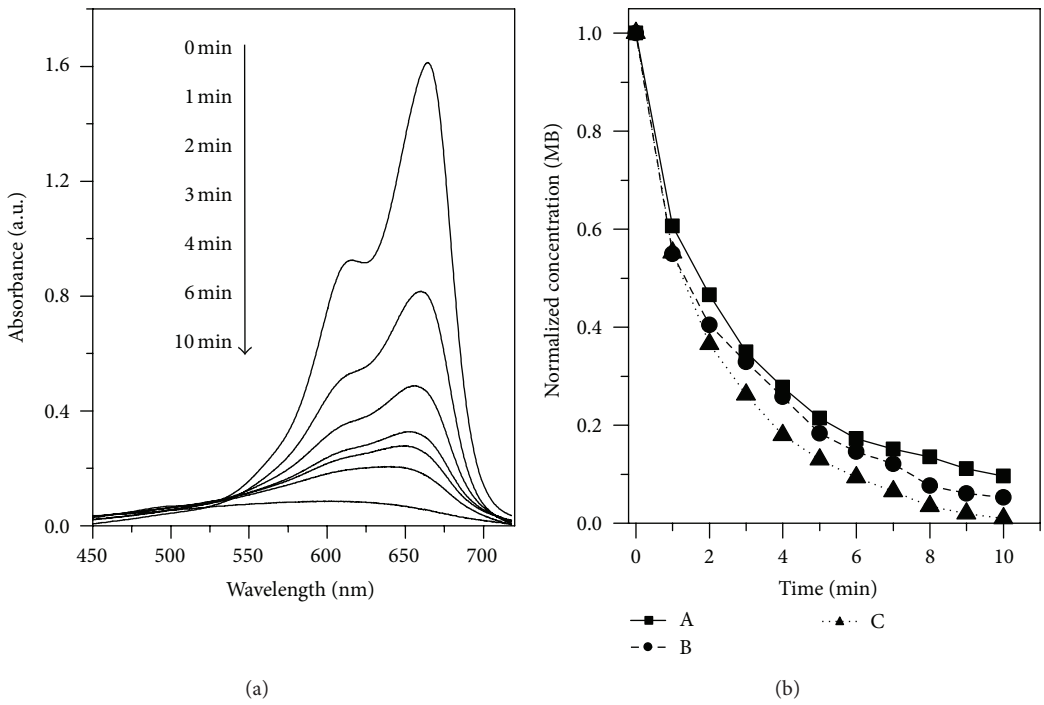


Figure 8: (a) The time dependent absorption spectra for CuS thin film vacuum annealed at 150°C and HP. (b) Change in the concentration of MB under different experimental conditions. Absorption spectra of A only have hydrogen peroxide, B thin film of the CuS without annealing and HP, C thin film, and CuS with annealing at 150°C and HP.

were 1.98, 2.07, and 2.34 eV for $T_a$ = 100, 150, and 200°C, respectively. These $E_g$ values are in agreement with values reported by other authors [43]. Generally, an increase in the gap of chemically deposited thin films is attributed to the band filling due to the Brustein-Moss effect in the valence band that in turn could affect the band gap of the layers. This cannot be attributed to a phase change, because in the range of annealing temperature studied, a phase change was not observed, by XRD or EDS techniques.

Table 1 shows the results of the chemical and physical properties reported in the literature. Copper sulfide has been obtained by a variety of techniques and consequently different properties are obtained. At the end of the table are the results obtained in the present research work in order to be compared with the results of other researchers. Our time to obtain the CuS is the fastest, only one hour compared to other processes, which are up to 40 hours by the same technique (CBD). The band gaps are within those reported in the literature for the CuS as shown in Table 1. The substrate temperatures ($T_s$) varied from 30 to 500°C (40°C in the present work); this also shows that when obtaining CuS thin films at temperatures below 100°C, heat treatments have been performed at 100–400°C.

Regarding the values obtained on electrical properties such as resistivity, mobility, carriers concentration, and activation energy ($\Delta E_a$), Adelifard et al. [7] obtained resistivity values better than those obtained in the present work ($1.93 \times 10^{-4}$ Ω-cm); this value was obtained by spray pyrolysis technique at a substrate temperature of 310°C. Nair et al. [27] obtained better resistivity values of $2.8 \times 10^{-4}$ Ω-cm; the technique was CBD (6–8 h) and an annealed treatment of 200–400°C. The mobility values obtained in the present work are among the best values obtained by other researchers; these values were obtained by expensive techniques such as sputtering, MOCVD, and spray pyrolysis. The activation energy values are very comparable to those obtained by He et al. [6] and Erokhina et al. [9]. On the other hand, we have obtained CuS thin films by an economical, simple (CBD), and fast (1 h) technique, with good electrical and optical properties, which could be applied in absorbing coatings, selective radiation filters in architectural windows, electrodes, chemical sensors, optoelectronic devices, and catalysts.

In order to show the prospective application as photocatalytic material, the CuS nanodisks thin films were used as catalysts in the degradation of methylene blue (MB) in the presence of hydrogen peroxide (HP) under germicidal light ($\lambda$ = 252 nm) at room temperature. Figure 8(a) displays the absorption spectra of aqueous solution of MB at different intervals in the presence of the sample annealed at 150°C and HP. The concentration was quantified considering the absorption at 653 nm. The absorption is time dependent and the complete mineralization of the MB was reached at 10 minutes for the experimental conditions described above.

As comparison values, for A in Figure 8(b) thesevalues correspond to an MB solution with HP, values for B to CuS thin film with HP and without annealing, and C corresponds to CuS with $T_a$ of 150°C and with HP. The photocatalytic activity of the CuS films with annealing at 100 and 200°C is not shown because their photocatalytic activity was lower than the ones for the films annealed at 150°C. The films

Table 1: Physical parameters of the $Cu_xS$ films reported in the literature.

| GDM | $E_g$ (eV) | $D$ (nm) | Ts (°C) | Ta (°C) | $d$ (nm) | $\rho$ (Ω·cm)<br>$\mu$ ($cm^2\ V^{-1}\ s^{-1}$)<br>$p$ ($cm^3$) | ΔEa (eV) | Phase | Reference |
|---|---|---|---|---|---|---|---|---|---|
| CBD<br>5–40 h | 1.3–1.45 | — | 50 | 200 | 300 | —<br>—<br>— | — | $Cu_{0.8}S$ | [1] |
| RF<br>— | — | — | 500 | — | 50–600 | 0.8–0.04<br>4–10<br>$1 \times 10^{18}$–$3 \times 10^{19}$ | 0.1–0.004 | $Cu_2S$<br>CuS | [6] |
| SP<br>— | 2.42–2.60 | 25.5–29.4 | 260–310 | — | 280 | $1.93–30 \times 10^{-4}$<br>12–25<br>$1.8 \times 10^{20}$–$1.7 \times 10^{21}$ | — | CuS | [7] |
| CBD<br>9–24 h | 2.48–2.90 | 2-3 | — | — | 70–233 | $1 \times 10^{8}$–$10^{6}$<br>—<br>— | 0.16–0.08 | CuS | [9] |
| PCD<br>1-2 h | 2.15–2.53 | — | RT | — | 150–350 | —<br>—<br>— | — | CuS<br>CuxS | [21] |
| MOD<br>— | 2.8 | 15–18 | RT | 350 | 300 | $3 \times 10^{5}$<br>1.72–16<br>$10^{12}$–$10^{15}$ | — | CuS | [25] |
| MOCVD<br>4–8 h | 2 | — | 300–500 | — | 20–2800 | 43–340<br>4<br>$1.3 \times 10^{17}$ | — | $Cu_xS$ | [26] |
| CBD<br>6–8 h | 1.4–1.55 | 11–20 | 25–70 | 200–400 | 500 | $2.8 \times 10^{-4}$<br>$23.5 \times 10^{-5}$<br>— | — | $Cu_xS$ | [27] |
| ASP<br>— | 2.2 | — | 270 | — | 320 | $6.25–3.13 \times 10^{-2}$<br>3.2–4.2<br>$2.3–6.2 \times 10^{19}$ | — | $Cu_2S$ | [30] |
| SP<br>— | 2.2 | — | 150–210 | — | 250 | —<br>—<br>— | — | CuS | [31] |
| CBD<br>18–20 h | 3 | 10–15 | 30 | — | 600 | —<br>—<br>— | — | CuS | [33] |
| CBD<br>1 h | 1.98–2.34 | 13.5 ± 3.5 | 40 | 100–200 | 378–733 | $8.25 \times 10^{-1}$–$1.72 \times 10^{-2}$<br>0.17–3.5<br>$6.25 \times 10^{18}$–$1.37 \times 10^{21}$ | 0.007–<br>0.013 | CuS | PS |

CBD: chemical bath deposition; RF: reactive sputtering; SP: spray pyrolysis; SDM: sorption diffusion method; PCD: photochemical deposition; MOD: metal organic deposition; MOCVD: metal organic chemical vapor deposition; ASP: aerosol assisted spray pyrolysis; GDM: growth deposition method; $D$: grain size; Ts: substrate temperature; Ta: annealing temperature; $d$: thickness; ΔEa: activation energy; PS: present Study.

for $T_a$ = 150°C with HP and irradiation show the better degradation of MB indicating that this combination plays a specific role in the degradation of MB. These results further indicate that the degradation of MB was enhanced as a result of the thermal vacuum annealing. Irradiation of the CuS thin films as well as HP may promote the formation of the $OH^{\bullet}$ species that is highly reactive and therefore the fast mineralization of MB as shown in Figures 8(a) and 8(b).

The improvement of the photobleaching of MB in presence of CuS thin films and HP could be explained as follows: the illumination of the semiconductor (CuS) produces charge carriers ($e^-$ and $h^+$) on the surface which participated in the redox reaction for generating $OH^{\bullet}$ radicals initializing the degradation of MB. The HP is a more highly oxidizing molecule than oxygen; thereby it contributes to a more efficient formation of hydroxyl radicals. On the other hand the HP contributes to the enhancement of the MB molecule destruction [44, 45]. The highly porous aspect of the material also is helpful for a more efficient photocatalytic activity. Further study is needed to clear, in a more detailed study, the effect of vacuum-annealed CuS on the photocatalytic reaction.

## 4. Conclusions

Simple and economical syntheses of CuS nanodisks were obtained. The resistivity, Hall mobility and carrier concentration measurements are dependent on the vacuum annealing temperatures. The transmittance was >60%. All the films showed semiconductor behavior with a type-p character for $32 \leq 1/k_BT \leq 40$ and a metallic nature for $1/k_BT < 31$ ($T < 100$°C). The better photodegradation of the MB occurred for a CuS vacuum-annealed thin film at 150°C in the presence of hydrogen peroxide.

## Acknowledgments

The authors thank the National Nanotechnology Laboratory located at CIMAV, Chihuahua, Mexico, for the use of electron microscopes and thank C. Ornelas for his valuable technical support.

## References

[1] P. K. Nair and M. T. S. Nair, "Chemically deposited SnS-$Cu_xS$ thin films with high solar absorptance: new approach to all-glass tubular solar collectors," *Journal of Physics D*, vol. 24, no. 1, pp. 83–87, 1991.

[2] D. M. Mattox and R. R. Sowell, "High absorptivity solar absorbing coatings," *Journal of Vacuum Science & Technology*, vol. 11, no. 4, pp. 793–796, 1974.

[3] S. B. Gadgil, R. Thangaraj, J. V. Iyer, A. K. Sharma, B. K. Gupta, and O. P. Agnihotri, "Spectrally selective copper sulphide coatings," *Solar Energy Materials*, vol. 5, no. 2, pp. 129–140, 1981.

[4] P. J. Sebastian, O. Gomez-Daza, J. Campos, L. Baños, and P. K. Nair, "The structural, transport and optical properties of screen printed $Cu_xS$ thick films," *Solar Energy Materials and Solar Cells*, vol. 32, no. 2, pp. 159–168, 1994.

[5] S. Lindroos, A. Arnold, and M. Leskelä, "Growth of CuS thin films by the successive ionic layer adsorption and reaction method," *Applied Surface Science*, vol. 158, no. 1, pp. 75–80, 2000.

[6] Y. B. He, A. Polity, I. Österreicher et al., "Hall effect and surface characterization of $Cu_2S$ and CuS films deposited by RF reactive sputtering," *Physica B*, vol. 308–310, pp. 1069–1073, 2001.

[7] M. Adelifard, H. Eshghi, and M. M. B. Mohagheghi, "An investigation on substrate temperature and copper to sulphur molar ratios on optical and electrical properties of nanostructural CuS thin films prepared by spray pyrolysis method," *Applied Surface Science*, vol. 258, no. 15, pp. 5733–5738, 2012.

[8] M. T. S. Nair and P. K. Nair, "SnS—$Cu_xS$ thin-film combination: a desirable solar control coating for architectural and automobile glazings," *Journal of Physics D*, vol. 24, no. 3, pp. 450–453, 1991.

[9] S. Erokhina, V. Erokhin, C. Nicolini, F. Sbrana, D. Ricci, and E. di Zitti, "Microstructure origin of the conductivity differences in aggregated CuS films of different thickness," *Langmuir*, vol. 19, no. 3, pp. 766–771, 2003.

[10] A. Šetkus, A. Galdikas, A. Mironas et al., "Properties of $Cu_xS$ thin film based structures: influence on the sensitivity to ammonia at room temperatures," *Thin Solid Films*, vol. 391, no. 2, pp. 275–281, 2001.

[11] A. U. Ubale, D. M. Choudhari, J. S. Kantale et al., "Synthesis of nanostructured $Cu_xS$ thin films by chemical route at room temperature and investigation of their size dependent physical properties," *Journal of Alloys and Compounds*, vol. 509, no. 37, pp. 9249–9254, 2011.

[12] X. P. Shen, H. Zhao, H. Q. Shu, H. Zhou, and A. H. Yuan, "Self-assembly of CuS nanoflakes into flower-like microspheres: synthesis and characterization," *Journal of Physics and Chemistry of Solids*, vol. 70, no. 2, pp. 422–427, 2009.

[13] D. Jiang, W. Hu, H. Wang, B. Shen, and Y. Deng, "Synthesis, formation mechanism and photocatalytic property of nanoplate-based copper sulfide hierarchical hollow spheres," *Chemical Engineering Journal*, vol. 189-190, pp. 443–450, 2012.

[14] J. Liu and D. Xue, "Solvothermal synthesis of CuS semiconductor hollow spheres based on a bubble template route," *Journal of Crystal Growth*, vol. 311, no. 3, pp. 500–503, 2009.

[15] D. J. Chakrabarti and D. E. Laughlin, "The Cu-S (Copper-Sulfur) system," *Bulletin of Alloy Phase Diagrams*, vol. 4, no. 3, pp. 254–271, 1983.

[16] R. J. Goble, "The relationship between crystal structure, bonding and cell dimensions in the copper sufides," *Canadian Mineralogist*, vol. 23, no. 1, pp. 61–76, 1985.

[17] D. F. A. Koch and R. J. McIntyre, "The application of reflectance spectroscopy to a study of the anodic oxidation of cuprous sulphide," *Journal of Electroanalytical Chemistry*, vol. 71, no. 3, pp. 285–296, 1976.

[18] S. R. Das, V. D. Vankar, P. Nath, and K. L. Chopra, "The preparation of $Cu_2S$ films for solar cells," *Thin Solid Films*, vol. 51, no. 2, pp. 257–264, 1978.

[19] D. Selle and J. Maege, "Elektrische und optische Eigenschaften von $Cu_2S$-Aufdampfschichten," *Physica Status Solidi B*, vol. 30, no. 2, pp. k153–k155, 1968.

[20] Z. Cheng, S. Wang, D. Si, and B. Geng, "Controlled synthesis of copper sulfide 3D nanoarchitectures through a facile hydrothermal route," *Journal of Alloys and Compounds*, vol. 492, no. 1-2, pp. L44–L49, 2010.

[21] J. Podder, R. Kobayashi, and M. Ichimura, "Photochemical deposition of $Cu_xS$ thin films from aqueous solutions," *Thin Solid Films*, vol. 472, no. 1-2, pp. 71–75, 2005.

[22] J. Z. Xu, S. Xu, J. Geng, G. X. Li, and J. J. Zhu, "The fabrication of hollow spherical copper sulfide nanoparticle assemblies with 2-hydroxypropyl-$\beta$-cyclodextrin as a template under sonication," *Ultrasonics Sonochemistry*, vol. 13, no. 5, pp. 451–454, 2006.

[23] X. H. Liao, N. Y. Chen, S. Xu, S. B. Yang, and J. J. Zhu, "A microwave assisted heating method for the preparation of copper sulfide nanorods," *Journal of Crystal Growth*, vol. 252, no. 4, pp. 593–598, 2003.

[24] S. Thongtem, C. Wichasilp, and T. Thongtem, "Transient solid-state production of nanostructured CuS flowers," *Materials Letters*, vol. 63, no. 28, pp. 2409–2412, 2009.

[25] S. K. Maji, N. Mukherjee, A. K. Dutta et al., "Deposition of nanocrystalline CuS thin film from a single precursor: structural, optical and electrical properties," *Materials Chemistry and Physics*, vol. 130, no. 1-2, pp. 392–397, 2011.

[26] R. Nomura, K. Miyawaki, T. Toyosaki, and H. Matsuda, "Preparation of copper sulfide thin layers by a single source MOCVD process," *Chemical Vapor Deposition*, vol. 2, no. 5, pp. 174–179, 1996.

[27] M. T. S. Nair, L. Guerrero, and P. K. Nair, "Conversion of chemically deposited CuS thin films to $Cu_{1.8}S$ and $Cu_{1.96}S$ by annealing," *Semiconductor Science and Technology*, vol. 13, no. 10, pp. 1164–1169, 1998.

[28] P. Roy, K. Mondal, and S. K. Srivastava, "Synthesis of twinned CuS nanorods by a simple wet chemical method," *Crystal Growth and Design*, vol. 8, no. 5, pp. 1530–1534, 2008.

[29] L. A. Isac, A. Duta, A. Kriza, I. A. Enesca, and M. Nanu, "The growth of CuS thin films by Spray Pyrolysis," *Journal of Physics*, vol. 61, no. 1, pp. 477–481, 2007.

[30] S. Schneider, Y. Yang, and T. J. Marks, "Growth of highly oriented chalcocite thin films on glass by aerosol-assisted spray pyrolysis using a new single-source copper thiolate precursor," *Chemistry of Materials*, vol. 17, no. 17, pp. 4286–4288, 2005.

[31] C. Nașcu, I. Pop, V. Ionescu, E. Indrea, and I. Bratu, "Spray pyrolysis deposition of CuS thin films," *Materials Letters*, vol. 32, no. 2-3, pp. 73–77, 1997.

[32] T. Y. Ding, M. S. Wang, S. P. Guo, G. C. Guo, and J. S. Huang, "CuS nanoflowers prepared by a polyol route and their

photocatalytic property," *Materials Letters*, vol. 62, no. 30, pp. 4529–4531, 2008.

[33] N. Mukherjee, A. Sinha, G. G. Khan, D. Chandra, A. Bhaumik, and A. Mondal, "A study on the structural and mechanical properties of nanocrystalline CuS thin films grown by chemical bath deposition technique," *Materials Research Bulletin*, vol. 46, no. 1, pp. 6–11, 2011.

[34] L. Y. Zhu, Y. Xie, X. W. Zheng et al., "Fabrication of novel urchin-like architecture and snowflake-like pattern CuS," *Journal of Crystal Growth*, vol. 260, no. 3-4, pp. 494–499, 2004.

[35] T. H. Larsen, M. Sigman, A. Ghezelbash, R. C. Doty, and B. A. Korgel, "Solventless synthesis of copper sulfide nanorods by thermolysis of a single source thiolate-derived precursor," *Journal of the American Chemical Society*, vol. 125, no. 19, pp. 5638–5639, 2003.

[36] M. B. Sigman Jr., A. Ghezelbash, T. Hanrath et al., "Solventless synthesis of monodisperse $Cu_2S$ nanorods, nanodisks, and nanoplatelets," *Journal of the American Chemical Society*, vol. 125, no. 51, pp. 16050–16057, 2003.

[37] J. H. Warner, M. H. Rümmeli, T. Gemming, B. Büchner, and A. D. Briggs, "Direct imaging of rotational stacking faults in few layer graphene," *Nano Letters*, vol. 9, no. 1, pp. 102–106, 2009.

[38] F. J. Lopez, E. R. Hemesath, and L. J. Lauhon, "Ordered stacking fault arrays in silicon nanowires," *Nano Letters*, vol. 9, no. 7, pp. 2774–2779, 2009.

[39] Y. M. Lu, W. S. Hwang, J. S. Yang, and H. C. Chuang, "Properties of nickel oxide thin films deposited by RF reactive magnetron sputtering," *Thin Solid Films*, vol. 420-421, pp. 54–61, 2002.

[40] Z. Xuping and C. Guoping, "The microstructure and electrochromic properties of nickel oxide films deposited with different substrate temperatures," *Thin Solid Films*, vol. 298, no. 1-2, pp. 53–56, 1997.

[41] D. A. Neamen, *Semiconductor Physics & Devices*, Irwin, 2nd edition, 1997.

[42] M. Ristov, G. Sinadinovski, I. Grozdanov, and M. Mitreski, "Chemical deposition of TIN(II) sulphide thin films," *Thin Solid Films*, vol. 173, no. 1, pp. 53–58, 1989.

[43] A. E. Pop, V. Popescu, M. Danila, and M. N. Batin, "Optical properties of $CU_xS$ nano-powders," *Chalcogenide Letters*, vol. 8, no. 6, pp. 363–370, 2011.

[44] D. F. Ollis, E. Pelizzetti, and N. Serpone, "Destruction of water contaminants," *Environmental Science and Technology*, vol. 25, no. 9, pp. 1523–1529, 1991.

[45] I. A. Salem and M. S. El-Maazawi, "Kinetics and mechanism of color removal of methylene blue with hydrogen peroxide catalyzed by some supported alumina surfaces," *Chemosphere*, vol. 41, no. 8, pp. 1173–1180, 2000.